Supporting information for:

Compound-Specific Radiocarbon Analysis of Low Molecular Weight Dicarboxylic Acids in Ambient Aerosols Using Preparative Gas Chromatography：Method Development

Buqing Xu[†‡], Zhineng Cheng[†*], Örjan Gustafsson[§], Kimitaka Kawamura[#], Biao Jin[†], Sanyuan Zhu [†], Tiangang Tang[†], Bolong Zhang[†], Jun Li[†], Gan Zhang[†*]

[†]State Key Laboratory of Organic Geochemistry and Guangdong-Hong Kong-Macao Joint Laboratory for Environmental Pollution and Control, Guangzhou Institute of Geochemistry, Chinese Academy of Sciences, Guangzhou 510640, China.

[‡] University of Chinese Academy of Sciences, Beijing 100049, China.

[§]Department of Environment Science and the Bolin Centre for Climate Research, Stockholm University, Stockholm, Sweden.

[#]Chubu Institute for Advanced Studies, Chubu University, Kasugai 487-8501, Japan.

*Corresponding Author: Dr. Gan Zhang

Tel: +86-20-85290805; fax: +86-20-85290706; e-mail: zhanggan@gig.ac.cn

Corresponding Author: Dr. Zhineng Cheng

Tel: +86-20-38350480; fax: +86-20-85290706; e-mail: chengzhineng@gig.ac.cn

CONTENT

to graphitized sample size.

Figure S10. Map of the sampling site

Figure S11. Three-day backward trajectory analyses for sample collected over Heshan

Figure S12. An example HRGC trace for ambient aerosol samples before and after PCGC isolation.

Text S1. Materials and standards

Thirteen dicarboxylic acids were used as authentic standards to evaluate any changes in isotope composition during the entire experimental procedure. In order to ensure that the standards cover a range of radiocarbon contents, three standards of oxalic acid (NIST OxII, IAEA-C7, IAEA-C8, purchased from NIST, Gaithersburg, USA) with quite different consensus radiocarbon content were selected. Their radiocarbon ages have been determined and ascertained through multi-laboratory analyses. Among these, NIST OxII provided "modern" radiocarbon age (Fm =1.3407), IAEA-C7 and IAEA-C8 were standard materials of two different intermediate ages (Fm = 0.4953 and 0.1503, respectively). Additionally, 10 more species of diacids (C_3, C_4, C_5, C_6, C_7, C_8, C_9, C_{10}, C_{11}, C_{12}, see the manufacturer and corresponding compound names in Table S1) were analyzed in duplicate, using large sample sizes (~1 mg C), to constrain well the "original ^{14}C isotopic composition" to be used throughout the analytical method development. Nearly all reference diacid compounds had an infinite radiocarbon age (Fm < 0.0050), with exception of the sebacic acid (C_{10}) which had a modern radiocarbon age (Fm = 1.0702 ± 0.0036). Furthermore, a compound (n-C_{22} alkane, purchased from Sigma-Aldrich, St Louis, MO) with modern ^{14}C signal (Fm = 1.0524 ± 0.0058) was selected as an internal standard to track the PCGC isolation process, which is sensitive to fossil carbon contamination if any during the procedures. Specific information about the standards is described in Table S1. These diacid standards (C_2–C_{12}) were dissolved in methanol at a concentration of 2 μg/μl each. 100-500μl of the standard solution were spiked onto the blank quartz filter to approximate the concentration of oxalic acid in ambient aerosols. The spiked filter was extracted and the extracts were analyzed for the recovery and $^{13}C/^{14}C$ isotope composition of diacids.

Table S1. Materials and standards used for CSRA-diacid method development [a]

Compound	Abbreviation	Manufacturer	$\delta^{13}C_{TOC}$(‰)	$Fm^{14}C_{TOC}$ [b]	^{14}C age [b]
Oxalic	Ox II	NIST	-17.8 [c]	1.3407[c]	modern
Oxalic	IAEA-C7	NIST	-14.5 [c]	0.4953 [c]	5645 [c]
Oxalic	IAEA-C8	NIST	-18.3 [c]	0.1503 [c]	15225 [c]
Malonic	C_3	Alfa Aestar	-28.1±0.05	0.0044±0.0001	43590±230
Succinic	C_4	TCI	-26.4±0.06	0.0029±0.0004	47095±270
Glutaric	C_5	Chem Service	-26.0±0.08	0.0046±0.0003	43240±300
Adipic	C_6	TCI	-26.6±0.03	0.0030±0.0002	47230±230
Pimeric	C_7	Dr Ehrenstorfer	-31.1±0.03	0.0044±0.0001	43670±260
Phthalic	Ph (C_8)	Sigma-Alodrich	-28.4±0.05	0.0028±0.0001	47300±230
Azelaic	C_9	TCI	-25.9±0.2	0.0050±0.0001	42640±220
Decanedioic	C_{10}	TCI	-27.9±0.1	1.0702±0.0036	-510±25
Undecanedioic	C_{11}	TCI	-27.2±0.07	0.0035±0.0002	45435±330
Dodecanedioc	C_{12}	Acros Organics	-31.2±0.07	0.0050±0.0001	42530±200
Dibutyl oxalate	C_2BE	TCI	nd[d]	0.0034±0.0002	45660±370
Dibutyl malonate	C_3BE	TCI	nd	0.0034±0.0001	45700±340
Dibutyl succinate	C_4BE	TCI	nd	0.0036±0.0001	45270±260
Dibutyl adipate	C_6BE	TCI	nd	0.0032±0.0001	46110±380
Dibutyl decanedioate	C_{10}BE	TCI	nd	0.5986±0.0015	4120±25
Dibutyl phthalate	PhBE (C_8BE)	TCI	nd	0.0030±0.0001	46680±370
n-docosane	n-C_{22}	Sigma-Alodrich	-30.0±0.06	1.0524±0.0058	-353±23
10%BF_3-butanol	BuOH	Sigma-Alodrich	-29.8±0.02	0.0029±0.001	46995±184

[a] For 1-butanol, carbon isotopic results were analyzed five times repeatedly. For other standards, the $\delta^{13}C_{TOC}$ measurement was repeated three times, bulk ^{14}C was measured in duplicate. $\delta^{13}C$ and $Fm^{14}C$ results were given in relative to VPDB and NBS Oxalic Acid. [b] known Fm ^{14}C values and ^{14}C age were determined by AMS at large scale (1mg C) after graphitization. [c] Nominal values. [d] nd, not determined.

Text S2. Examine the derivatization steps for dicarboxylic acids

There are three parameters that will influence derivatization steps, (1) the volume of derivatizing reagent added into sample (2) reaction time for acid esterification and (3) reaction temperature for esterification. In order to test the best reaction conditions for diacids, we added 500μl of BF3/n-butanol to every sample and standard, which was thought to be excessive. A mixture solution contained 4 diacids (C_2, C_3, C_6, and C_{10}) was prepared into methanol with a concentration of 2μg/μl. The time for acid esterification was tested from 0 min to 90 min with heating temperature controlled at 80℃. The yields of the esters were tested by GC/FID through a set of standard solution of diacid dibutyl esters with different concentration. As shown in Figure S1a, the yields of the esters reach a peak value in 60min. when the reaction time continues to increase, C_2 went down but other diacids appear to be stable. In the same way, we tested the heating temperature for acid esterification from 30℃ to 120℃ with reaction time controlled at 60min (Figure S1b). The yields of the esters reach a plateau at100℃. In conclusion, heated at 100℃ for 60min was an optimal condition, that the recovery of C_2 was 82% and for other three diacids was better than 97%.

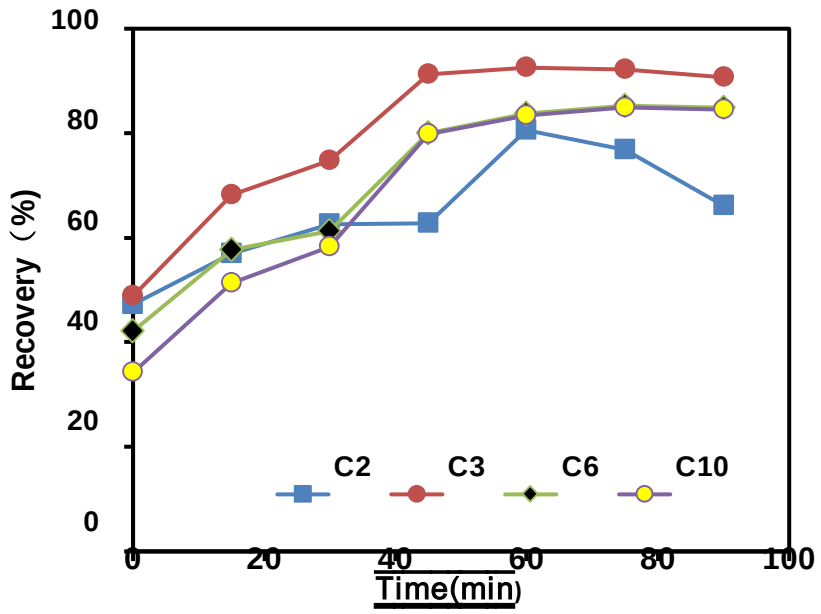

Figure S1a. Yields of dibutyl esters for diacid standards with reaction time.

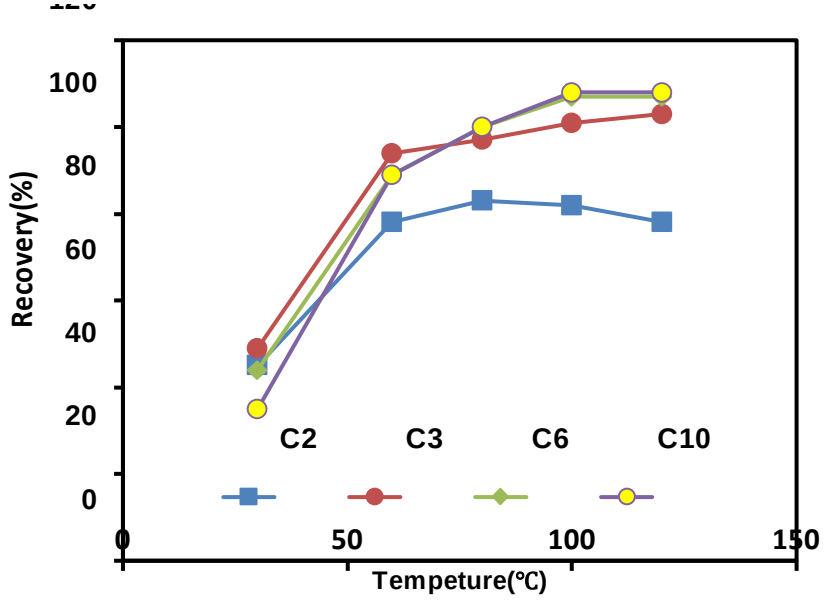

Figure S1b. Yields of dibutyl esters for diacid standards with reaction temperature.

Text S3. Optimization and performance of the PCGC system

The PCGC system used for separation of diacids consists of an Agilent 7890A gas chromatograph (GC) equipped with a flame ionization detector and an Agilent 7693 series injector. A cooled injection system (CIS) and Gerstel preparative fraction collector (PFC) were configured in the PCGC system (Figure S2). The GC was equipped with a widebore column with 5% phenyl -95% dimethyl polysiloxane stationary phase (DB-5MS, 30 m × 0.53 mm i.d., 1.5 μm film thickness, Agilent Technologies). Helium was used as a carrier gas at a constant flow of 5 ml/min. The PCGC oven temperature was programmed to increase from 50℃ to 160℃ at a rate of 30℃/min, and then to 280℃ at 5℃/min, and finally to 295℃ at 30℃/min with a hold for 3 min. The column connects to a zero dead volume effluent splitter to divert 1% of the eluting components to FID to monitor column effluent and 99% to the glass tube traps through preparative fraction collector.

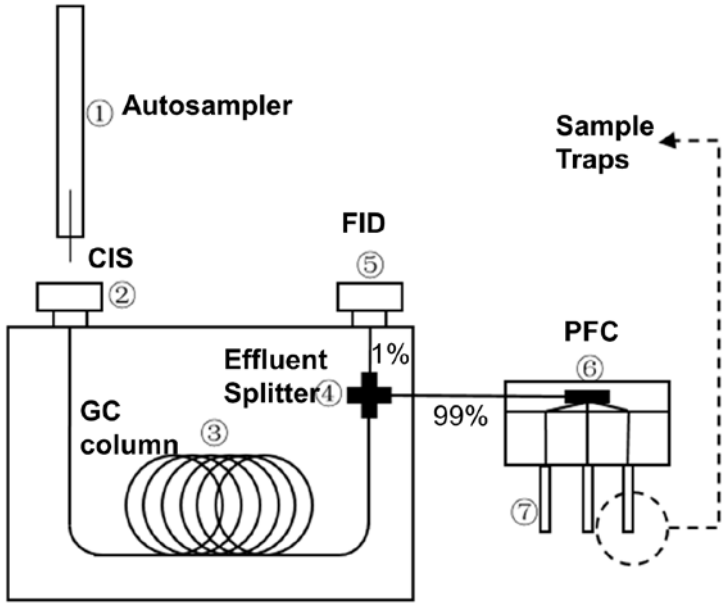

Figure S2. Diagrammatic representation of the PCGC instrument

This is the first work using a PCGC system for the isolation and harvesting of individual diacids. Hence, we optimized the PCGC conditions to obtain minimal peak area of solvent, maximum peak area of target compounds, and maximum harvesting recovery, respectively. The following instrumental parameters were evaluated in sequence: (1) CIS inlet initial temperature and final temperature, (2) CIS solvent

venting time, (3) CIS splitless time, (4) CIS injection rate, and (5) PFC trapping temperature. A mixture of diacids solution was derivatized and injected into PCGC, the signal intensity of each diacids was investigated by varying each parameter at a time and keep other parameters consistent. For the optimization experiments of the CIS operating parameters, the peak of diacids from each injection were normalized against the maximum peak area observed during the corresponding series of injection. The principle of the optimization was to obtain the highest signal intensity of each diacids, and to select the minimum solvent peak area on this basis. Each optimal value was applied in subsequent optimization experiments. For the optimization of PFC trapping temperature, three diacids were trapped under different temperature of glass trap. Figure S3a to Figure S3f showed the optimized results for each parameter. Briefly, the PCGC system was operated at the optimum conditions for diacids. (a) CIS: autoinjector “fast injection” mode, CIS “solvent vent” mode, 6 s of solvent venting time, 2 min CIS splitless time and CIS programming from 40°C (hold time: 0.1 min) to 300°C at a rate of 12°C/min, (b) GC: DB-5MS “megabore” fused-silica capillary column (30 m × 0.53 mm i.d., 1.5 μm film thickness) and oven temperature programming from 50°C to 160°C at a rate of 30°C/min, and to 280°C at a rate of 5°C/min, finally to 295°C at 30°C/min (hold 3 min) at a rate of 30°C/min, (c) PFC: 300°C PFC switch temperature and 20°C (ambient) PFC trapping temperature.

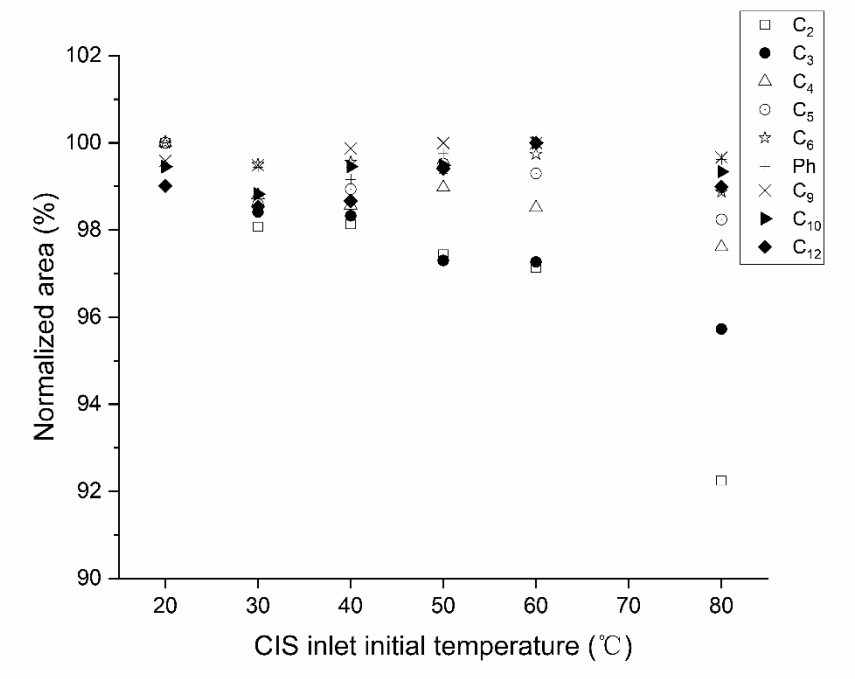

Figure S3a. Relative area counts for nine Derivative diacids as a function of CIS inlet initial temperature (20℃-80℃). CIS inlet initial temperature should be set at 40℃ when the solvent was eliminated with the least loss of target analytes.

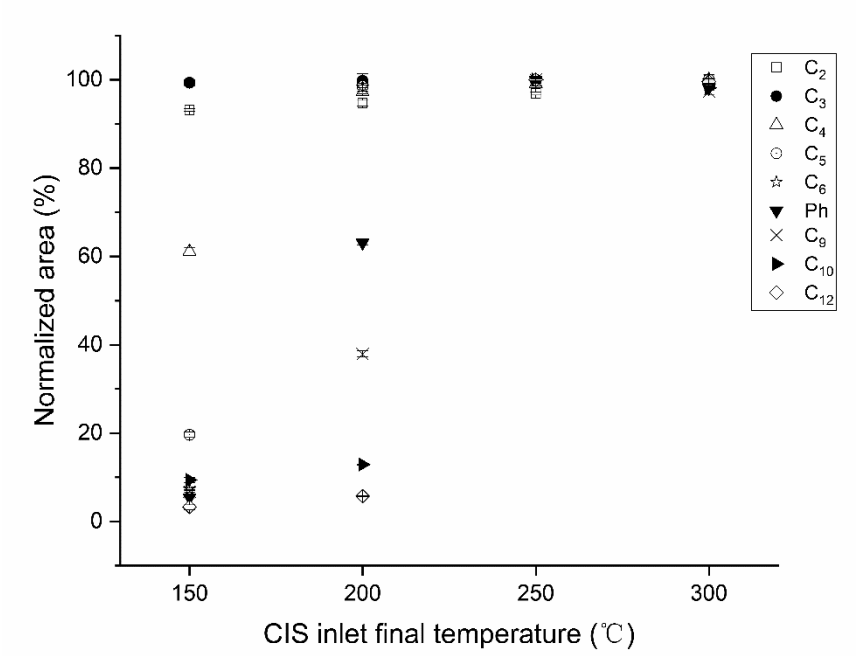

Figure S3b. Relative area counts for nine Derivative diacids as a function of CIS inlet final temperature (150℃-300℃). CIS inlet final temperature should be set at 300℃ when diacids with higher boiling points could evaporate into column

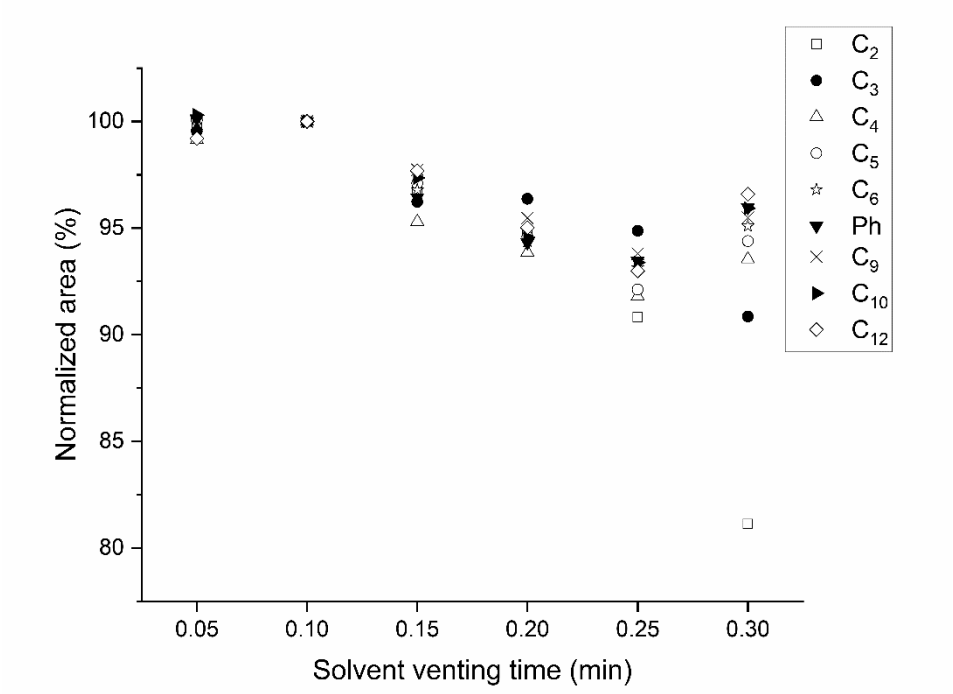

Figure S3c. Relative area counts for nine diacids as a function of solvent venting time (0.05 min- 0.3min). Solvent venting time should be set at 0.1min when the solvent was eliminated with the least loss of target analytes

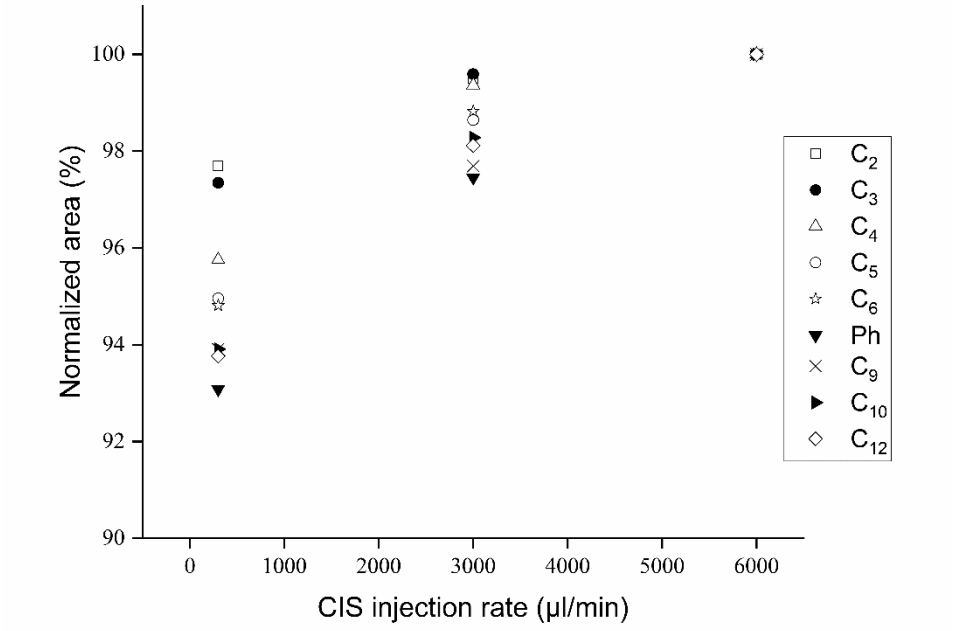

Figure S3d. Relative area counts for nine diacids as a function of different injected rate. The maximum injection speed (fast injection mode) should be selected

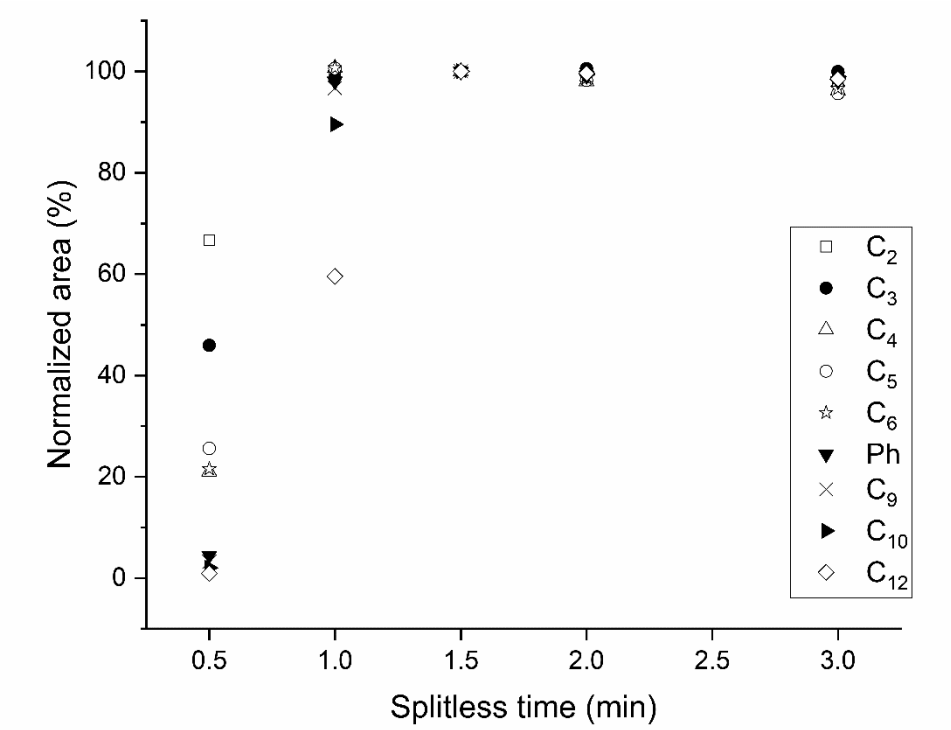

Figure S3e. Relative area counts for nine diacids as a function of CIS splitless time (0.5min-3min). A spitless time of 2min was chosen when diacids with higher boiling points could evaporate into column.

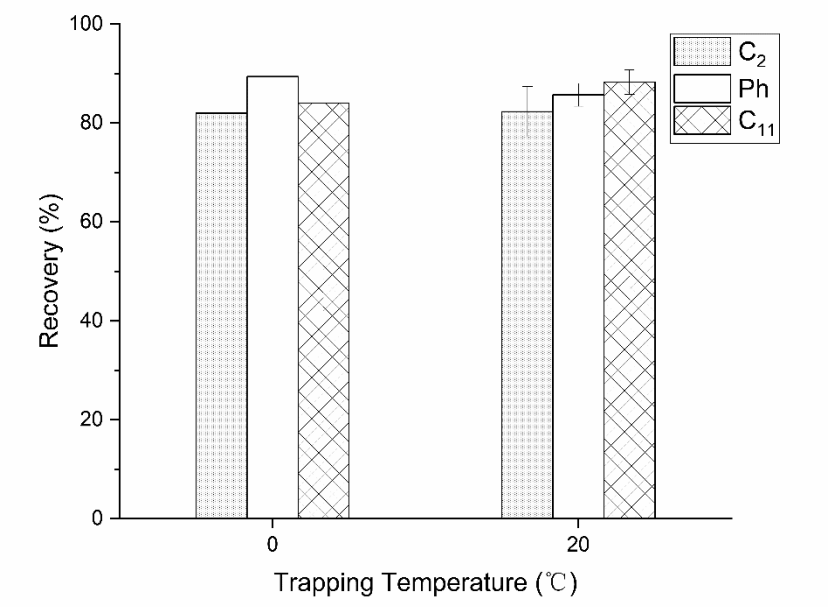

Figure S3f. Trapping recovery of three diacid esters as a function of trapping temperature of the preparative fraction collector (PFC). The error bars correspond to ±1 standard deviation(n=3). It suggest that harvesting diacids in ambient temperature (20℃) should be possible.

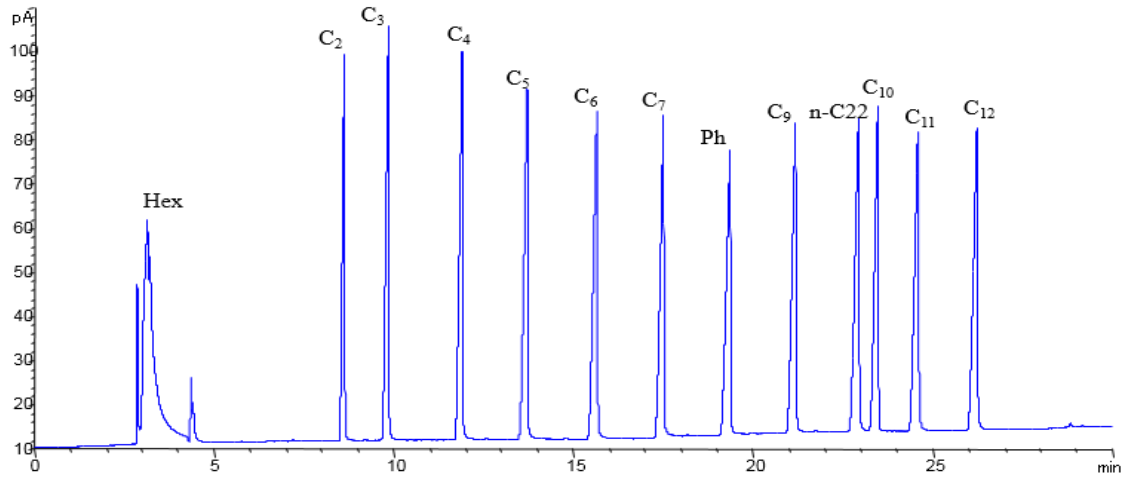

Figure S4. A typical PCGC chromatogram of mixture diacid standards. The diacid standards are defined in Table S1. The chromatogram represents the optimal PCGC conditions.

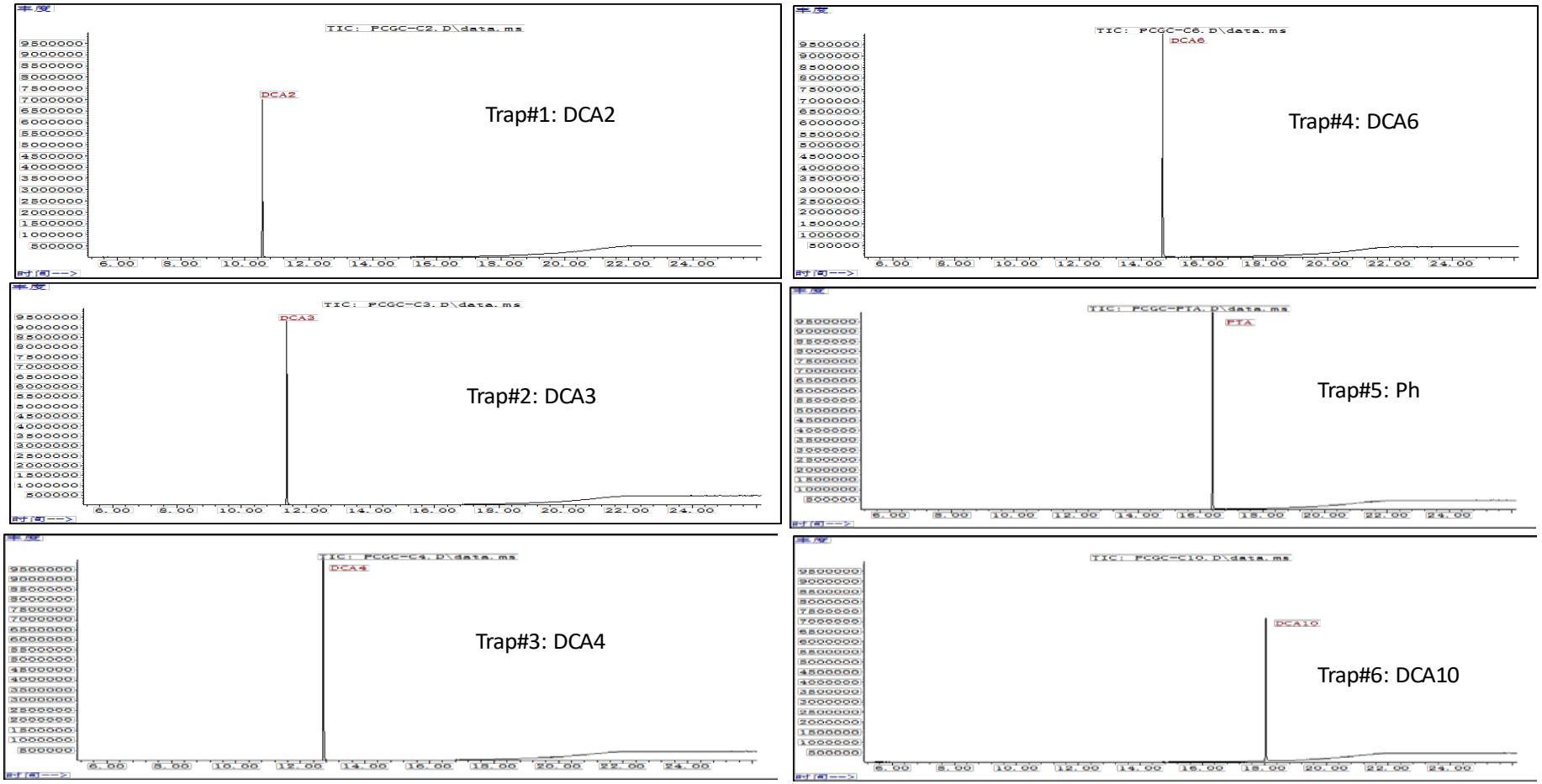

Figure S5. GC-MS traces of trapped diacid standards isolated by PCGC

Text S4. Evaluation of carbon contamination.

Carbon contamination amenable to gas chromatography was constrained by mass spectrometry (as described above) to be negligible, yet other contamination (e.g., residual solvent prior to graphitization, dust, column bleed, etc.) that also may induce conspicuous error in the resulting ^{14}C data，especially after the target compound was isolated by PCGC. Hence, current methodologies were assessed to characterize any significant process contamination.

Compared with other common solvents (e.g., acetone, hexane, methanol), dichloromethane has high volatility and low carbon content rate, which minimizes any solvent interference in ^{14}C analysis. Therefore, the trapped sample was dissolved in CH_2Cl_2 and transferred into a 100 μl tin cup, followed by solvent removal using a nitrogen blow-down system. Nitrogen blow-down time showed key effect on the solvent removal. The optimal N_2 processing time was constrained using constant flow rate and ambient temperature at 100 ml/min and 30℃, respectively. Dibutyl oxalate (C_2BE) standard was added with a known mass into a 100 μl tin cup, then the cup was filled with CH_2Cl_2 and dried under N_2 flow. Different N_2 blow-down times were assessed by comparing yields from combustion (manometric measurement of CO_2) versus the initial carbon mass (Figure S6). Preliminary experiments showed that the mass of C_2BE start to decrease after 5 min. However, solute tend to form a “skin” and wrap the residual solvent during N_2 blow-down. Hence, we choose 10 min blow down to process LMW diacids (C_2-C_{12}) consistently. Another similar experiment on n-docosane which has a higher boiling point (369 ℃) also demonstrated that 10 min is suitable (Figure S6). A size of 200 μgC of dibutyl decanedioate ($C_{10}BE$) was dissolved and dried repeatedly (n = 6) during N_2 blow-down for 10 min. Figure S7 revels that all Fm values from dried sample (average Fm = 0.5967 ± 0.0022) agree well with those from bulk combustion (average Fm = 0.5982 ± 0.0015). This result proved the absence of any fossil carbon contamination from residual solvent since the radiocarbon composition of $C_{10}BE$ (Fm = 0.5982) and solvent (Fm ≈ 0) differ sufficiently.

Another potential source of carbon contamination is “column bleed” from thermal

degradation of the chromatographic stationary phase. Carbon from column bleed are of "infinite" ^{14}C age due to the fossil carbon feedstock used in its production[1]. In order to evaluate "column bleed effect", six diacid dibutyl ester standards (C_2BE, C_3BE, C_4BE, C_6BE, C_8BE, $C_{10}BE$) were mixed and dissolved in hexane and each compound was isolated. Although no sample cleanup was performed, the individual Fm results for $C_{10}BE$ (Figure S7), the highest boiling-point material, indicated that bleeding of the stationary phase did not cause a negative carbon process contamination at the applied oven temperature (260℃). This result was consistent with the findings of Zencak et al., who used radiocarbon-modern vanillin to demonstrate the absence of any fossil C contamination in the sample processed by PCGC[2]. Furthermore, Casanova et al. showed that column bleed contamination from the PCGC was negligible through ^1H NMR analysis[1,3].

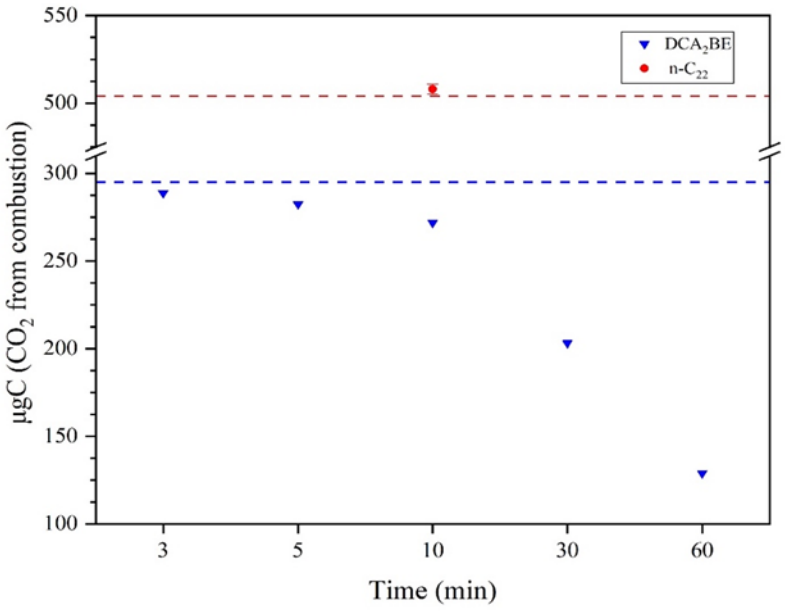

Figure S6. Changes of target compounds (CO_2 measured manometrically) under different nitrogen blowing time. Blue line represents the initial carbon content of C_2BE, red line represents the initial carbon content of n-C22.

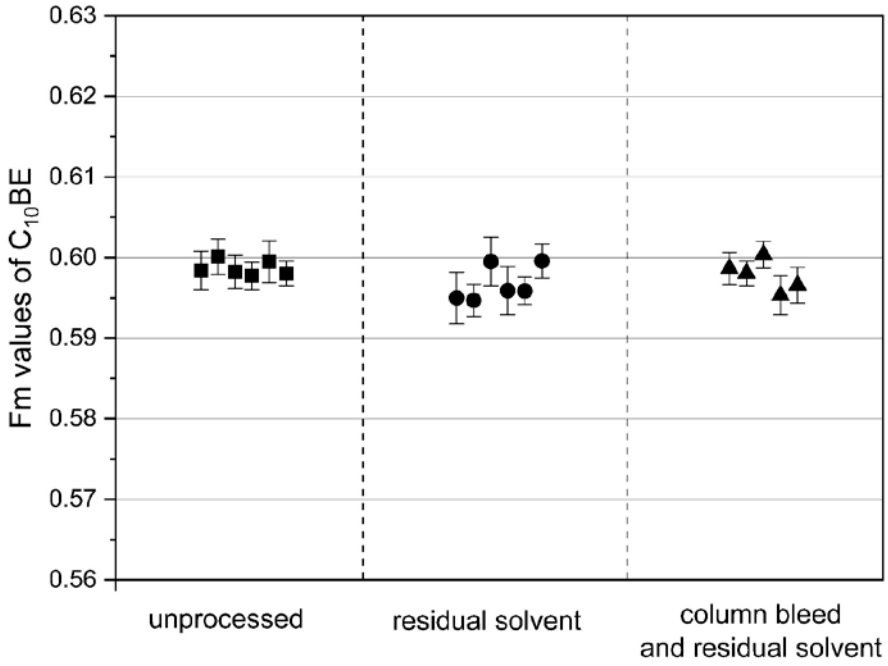

Figure S7. Tests of method-induced carbon contamination (Fm values of C_{10}BE standard). Squares represent unprocessed standards, circles represent standards treated by "solvent evaporation" process, triangles represent standards treated by both "PCGC isolation" and "solvent evaporation". All sample sizes in this figure are around 200 μg of C.

Text S5. Examination of potential isotopic fractionation

The effects of method-induced isotopic fractionation were evaluated by stable carbon isotope ($\delta^{13}C$) analysis of specific diacids using a gas chromatograph/isotope ratio mass spectrometer system (GC-IRMS). A method for the $\delta^{13}C$ analysis of specific dicarboxylic acids was described by Kawamura and Watanabe in 2004[4]. Diacids were in that study reacted with 1-butanol to derive dibutyl esters. After measuring the $\delta^{13}C$ value of butyl esters, $\delta^{13}C$ of diacids were calculated by an isotopic mass balance approach, using the isotopic composition of derived carbon. The $\delta^{13}C$ value of 1-butanol and authentic diacid (C_2-C_{12}) standard were determined using Flash 2000 elemental analyzer connected to an isotope ratio mass spectrometer (IRMS, Delta V, Thermo Scientific). The $\delta^{13}C$ values of derivatives were determined using GC ISOLink2/IRMS.

Potential points of the method where isotope fractionation may occur are during the esterification as well as in the PCGC (i.e., at the effluent splitter, chromatographic column, cryogenic traps, the primary cause would be incomplete collection)[5]. The first goal was to examine the isotope fractionation during esterification. Diacid standards were derivatized to their dibutyl esters and were repeatedly (n = 3) measured by GC/IRMS. The derivatizing reagent and 11 authentic diacid standards were also repeatedly (n = 3) measured to establish their original $\delta^{13}C$ values by EA/IRMS (Table S1). Table S2 presents calculated $\delta^{13}C$ values for the diacids component of the derivatives and the corresponding values of the unprocessed compounds. The differences were small and ranged from 0.04‰ to 0.73‰. Except for C_3 and C_9 (0.57‰ and 0.73‰, respectively), other diacids have a difference less than 0.5‰. These results are consistent with a previous study, in which a difference less than 0.71‰ was observed for LMW diacids and ketocarboxylic acids[4]. Therefore, the experimental results indicated that isotopic fractionation during the derivatization was negligible in this method.

Previous studies have observed that isotopic fractionation can occur as a result of PCGC isolation, likely because only a part of the entire target compound was collected[5,6]. It is essential to ensure that the trap window encompasses the entire peak

in PCGC isolation and collection of target analytes destined for off-line isotope analysis. The high reproducibility observed for both retention times and signal intensities help us to set narrow trapping time windows. Before PCGC isolation, the $\delta^{13}C$ values of 11 diacids were already measured directly by GC/IRMS as showed in Table S2. These compounds were then isolated from their mixed solution by PCGC. After isolation and collection, each individual diacids were also analyzed wih the same GC/IRMS method. Figure S8 presents $\delta^{13}C$ values of each target compound before and after PCGC isolation.

The carbon isotopomers of the target compounds generally became a little heavier after PCGC collection. It is well known that the $^{13}C/^{12}C$ ratio varies within GC conditions; heavy carbon isotopomers elute earlier than the lighter ones[7,8]. This may contribute to the slight enrichment of heavy isotopomers, and, accordingly, heavy isotopomers were observed in each target compounds trapped by PCGC. Fortunately, the differences between original and trapped $\delta^{13}C$ values are less than 0.5‰ during the PCGC isolation. The maximum offset was observed in C_7 with a bias of 0.47‰. The good agreement and limited isotope fractionation during entire PCGC procedure is described by the linear function, $y=0.98x - 0.45$, $R^2 = 0.98$.

Table S2. Evaluation of $\delta^{13}C$ fractionation of dicarboxylic acids during derivatization[a].

Compound	Measured $\delta^{13}C_{DiBE}$	Calculated $\delta^{13}C_{Diacid}$[b]	Original $\delta^{13}C_{Diacid}$[c]	Difference
C_2 (Ox Ⅱ)	-27.49±0.07	-18.27±0.37	-17.80	0.47
C_3	-29.17±0.11	-27.48±0.42	-28.05±0.05	-0.57
C_4	-28.58±0.11	-26.14±0.32	-26.44±0.06	-0.30
C_5	-28.21±0.14	-25.66±0.36	-25.98±0.08	-0.32
C_6	-28.50±0.06	-26.77±0.13	-26.61±0.03	0.16
C_7	-30.43±0.07	-31.16±0.16	-31.10±0.03	0.04
C_8	-29.33±0.10	-28.87±0.20	-28.40±0.02	0.47
C_9	-27.33±0.15	-25.14±0.28	-25.87±0.16	-0.73
C_{10}	-28.59±0.11	-27.62±0.20	-27.86±0.12	-0.24
C_{11}	-28.59±0.13	-27.72±0.22	-27.20±0.07	0.52

C_{12}	-30.53±0.32	-31.02±0.53	-31.23±0.07	-0.21

[a]GC-irMS analyses were performed in triplicate, the average values are given with standard deviation. [b]calculated by an isotopic mass balance using the $\delta^{13}C$ value of butyl esters and n-butanol. [c]original $\delta^{13}C$ values were described in Table S1

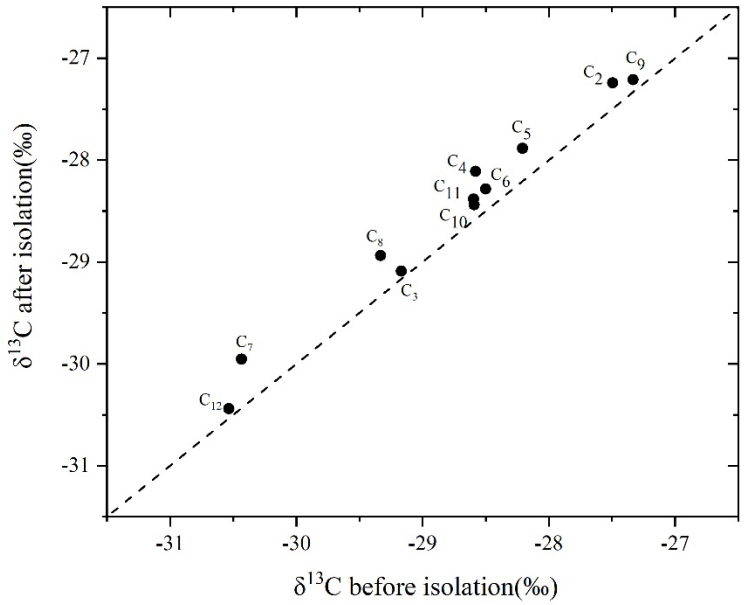

Figure S8. Comparison between $\delta^{13}C$ values of 11 diacids between and after isolation by PCGC. The solid and dashed lines represent regression line and 1:1 line.

Text S6. Quantification of procedural extraneous carbon

Isolation procedure carbon blanks are expected to be too small to be measured directly. To evaluate the negative/positive exogenous or nonspecific background carbon (C_{ex}), a pair of standards across a range of sample size with a modern or dead ^{14}C composition (n-docosane and phthalic acid) were applied. With the offsets between measured and original Fm results, modern carbon (MC) and dead carbon (DC) blank masses were determined by using this pair of standards having similar chromatographic behavior yet with contrasting ^{14}C content[2,9]. Isotopic offsets from the original Fm values of the modern n-docosane (the control compound was selected to be similar in properties to diacid esters) gave the DC contamination (hereafter DCC), whereas the MC contamination (hereafter MCC) was determined from the offset from the original

Fm values for the phthalic acid with dead ^{14}C composition. The Fm value of samples was expressed by the following equation:

$$Fm_{sample} \times C_{sample} = Fm_{measured} \times C_{measured} - Fm_{ex} \times C_{ex} \quad (1)$$

where C_{sample} is equivalent to $C_{measured}$-C_{ex}, and C_{ex} is DCC+MCC.

In this approach, n-docosane, which has a modern ^{14}C signal (Fm = 1.0524 ± 0.0058), was added to the mixture of 11 diacids, and was isolated across a range of sample sizes (25-250 μg of C) that corresponds to reasonable sample sizes for CSRA of oxalic acid in ambient aerosols. Similarly, phthalic acid, which has a dead ^{14}C signal (Fm = 0.0028 ± 0.0001), was also isolated across the same range of sample sizes (25-250 μg of C). Using the modern/dead carbon correction, it was resolved with fossil phthalic acid that 0.8±0.4 μg of modern-C (MCC, with assumed Fm_{ex} = 1.0) was added into the full sample processing, while the observed Fm values for modern docosane demonstrated that a similarly low value of 0.2 ± 0.1 μg of dead-C (DCC, with assumed Fm_{ex} = 0.0) also was added.

The size of DCC was much smaller than the MCC, which was also supported by the exhaustive evaporation of solvent and the negligible column bleed contamination as demonstrated above. Santos et al.[10] also reported that DCC is usually smaller than MCC for ordinary AMS-^{14}C sample processing. In their study, samples ＞0.1 mg show an average MCC of ＞0.7 μg C, while DCC contamination is typically 0.3 μg C. In conclusion, indirect analysis of the C_{ex} was 1.0 ± 0.5 μg C and Fm = 0.8 ± 0.4.

Text S7. Radiocarbon analysis of standard dicarboxylic acids

The Fm results for the procedural diacids, corrected for DC and MC blank mass, were compared with those of the independently measured “original” Fm values of unprocessed standards (Table S3). An isotopic mass balance approach was adopted to correct the carbon contribution of butanol groups (-C_4H_9) introduced in the derivatization of diacids, where appropriate:

$$Fm_{DABE} = f_{Diacid} \times Fm_{Diacid} + f_{BuOH} \times Fm_{BuOH} \quad (2)$$

where f_{Diacid} and f_{BuOH} are fractions of carbon in the esters derived from diacids and 1-butanol. The Fm^{14}C value of individual diacids (Fm_{Diacid}) was then calculated based on the values of the derivative (Fm_{DABE}) and 1-butanol (Fm_{BuOH}) that were measured by AMS.

The FM values of corrected samples were expressed by the following equation:

$$Fm_{corr} = \frac{Fm_{measure} \times C_{measure} - Fm_{ex} \times C_{ex}}{C_{measure} - C_{ex}} \quad (3)$$

The error associated with the Fm_{corr} is the propagated total uncertainty (σ) calculated as follows:[2,11]

$$\sigma = \sqrt{\sum_{i=1}^{n} \left(\frac{\partial Fm}{\partial x_i}\right) {\sigma_{x_i}}^2} \quad (4)$$

Where σ_{x_i} include the uncertainty for AMS uncertainty of Fm measured ($\sigma_{Fm_{measure}}$), the uncertainty for Fm_{ex} ($\sigma_{Fm_{ex}}$), the uncertainty for carbon masses of $C_{measured}$ and C_{ex} ($\sigma_{C_{measure}}$ and $\sigma_{C_{ex}}$, respectively).

For the nine ^{14}C-dead diacid standards, the measured Fm values without C_{ex} correction were a little higher than the original Fm values. After corrections, Fm values agree well with the expected ones (Table S3). Except for one standard compound (C_{12}), which had a slightly higher bias of 0.012 Fm, the offsets between Fm_{corr} and Fm_{orig} for other dead standards were less than ± 0.0066 (equivalent to 6.6‰). For example, the average Fm_{corr} value of C_7 is 0.0053±0.0005, which is very close to the expected Fm_{orig} values (0.0044 ± 0.0001). For the modern C_{10} diacid standard C_{10} the Fm_{corr} (average 1.0676 ± 0.0021) also agreed within 1σ with the Fm value measured from unprocessed material (1.0702 ± 0.0036).

The particular concern about the procedure for the preparative separation of oxalic acid from ambient aerosols and subsequent CSRA was further addressed. In order to verify the accuracy of our method for oxalic acid in aerosol samples that have mixed biological/fossil sources, we choose three kinds of artificial oxalic standards: NIST-OXII, IAEA C7 and IAEA C8, whose nominal Fm values are 1.3407, 0.4953 and 0.1503, respectively (Table S1). Table S3 indicates that the accuracy of the method was very

high since only a very small offset between corrected Fm and original Fm values was observed in replicate isolations and analyses of the oxalic acid standards (offsets ranged from Fm 0.0020 to 0.0197). Ultimately, the Fm_{corr} values in 36 out of 37 diacids examined fell within the 2σ range of their Fm_{orig} values, while the Fm_{corr} values in 28 out of 37 diacids examined fell into the 1σ range of their Fm_{orig} values (Table S3).

For environmental application of the CSRA-diacids method, uncertainty of the corrected values is also a consideration. It should be noted that the uncertainty will be enlarged by the contribution of the two butyl groups added to the derivatives of the diacids. Particularly for oxalic acid, which has the highest f_{BuOH} value (a fraction of the carbon in the derivatives originated from 1-butanol, f_{BuOH} = 0.8), the measurement uncertainty was enlarged by a factor of 5 after the correction. Fortunately, the sample size was also 5 times larger, which diminished the uncertainty associated with blank carbon correction. Our data showed a significant decrease in uncertainty with increasing sample size (Figure S9), this effect is predominately caused by the diminishing influence of the blank carbon contribution. For oxalic acid, a sample size of >100 μg of C yielded uncertainty of 1SD with total propagated error of < 0.02 Fm. For diacids with higher molecular weight, the increase in uncertainty caused by decreasing sample size was not significant. For example, we found that a graphitized sample size of ＞50 μg of C yield uncertainty of 1SD error less than 0.02 Fm for phthalic and C_{10}.

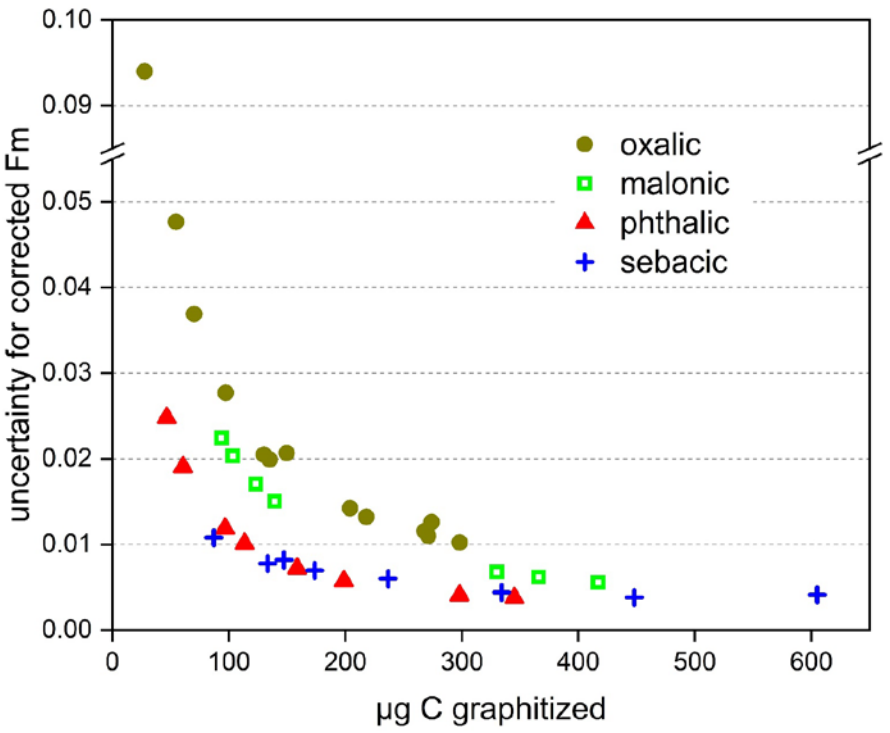

Figure S9. Relationship of total propagated uncertainty for corrected Fm values relative to graphitized sample size.

Table S3. Fm values determined for procedural diacids standard

Target compound	GIG Lab code	Inj [a]	Injection mass(μgC)[b]	Yield CO_2(μgC)[c]	Fm			
					Uncorrected	Corrected [d]	Original [e]	Difference [f]
Ox Ⅱ (C_2)	GIG201808070	55	352	135	1.3784±0.0087	1.3589±0.0199	1.34	0.0182*
	GIG201808037	63	414	274	1.3484±0.009	1.3387±0.0126		-0.002*
	GIG201808030	51	208	150	1.3644±0.0128	1.3468±0.0206		0.0061*
IAEA-C7 (C_2)	GIG201808059	48	340	298	0.5267±0.005	0.515±0.0102	0.5	0.0197**
	GIG201808062	41	290	268	0.5115±0.0059	0.4985±0.0116		0.0032*
	GIG201808063	38	269	218	0.5194±0.005	0.5034±0.0132		0.0081*
IAEA-C8 (C_2)	nd	36	255	nd [g]	nd	nd	0.15	nd
	GIG201808060	37	262	204	0.1564±0.0039	0.1375±0.0142		-0.0128*
	GIG201808061	40	283	271	0.1596±0.0039	0.1454±0.011		-0.0049*
C_3	GIG201808031	51	419	366	0.0102±0.0025	0.0023±0.0062	0.0044±0.0001	-0.0021*
	GIG201808038	63	715	417	0.0101±0.0025	0.0031±0.0056		-0.0013*
	GIG201808065	55	375	330	0.0181±0.0025	0.0092±0.0068		0.0048*
C_4	GIG201808032	51	369	315	0.0039±0.002	-0.0037±0.0058	0.0029±0.0004	-0.0066**
	GIG201808039	63	692	335	0.0125±0.0021	0.0054±0.0055		0.0025*
	GIG201808066	55	361	344	0.0105±0.002	0.0035±0.0053		0.0006*
C_5	GIG201808016	79	633	315	0.0142±0.0018	0.0076±0.005	0.0046±0.0003	0.003*
	GIG201808023	54	403	333	0.0153±0.0018	0.0091±0.0048		0.0045*
	GIG201808044	54	396	316	0.0137±0.0018	0.0072±0.005		0.0026*

C_6	GIG201808033	51	440	410	0.0017±0.0016	-0.0029±0.0036		-0.0059**
	GIG201808040	63	731	666	0.0053±0.0002	0.0025±0.002	0.0030±0.0002	-0.0005*
	GIG201808067	55	349	342	0.0048±0.0016	-0.0007±0.0042		-0.0037*
C_7	GIG201808017	79	602	471	0.0085±0.0015	0.0049±0.003		0.0005*
	GIG201808024	54	384	311	0.0113±0.0015	0.0058±0.0042	0.0044±0.0001	0.0014*
	GIG201808045	54	377	316	0.0105±0.0015	0.0051±0.0041		0.0007*
C_8	GIG201808068	55	305	298	0.0034±0.0014	-0.0019±0.004		-0.0047**
	GIG201808041	63	795	711	0.005±0.0003	0.0028±0.0016	0.0028±0.0001	0.0000*
	GIG201808034	51	342	345	0.0067±0.0018	0.0021±0.0037		-0.0007*
C_9	nd	79	581	nd	nd	nd		nd
	GIG201808025	54	370	286	0.0079±0.0013	0.0026±0.004	0.0050±0.0001	-0.0024*
	GIG201808046	54	364	275	0.0039±0.0013	-0.0016±0.0041		-0.0066**
C_{10}	GIG201808035	51	529	448	1.0661±0.0034	1.0652±0.0038		-0.005*
	GIG201808042	63	803	605	1.0696±0.0039	1.069±0.0041	1.0702±0.0036	-0.0012*
	GIG201808069	55	316	334	1.0698±0.0038	1.0687±0.0044		-0.0015*
C_{11}	GIG201808019	79	565	428	0.0036±0.0012	0.0003±0.0026		-0.0032**
	GIG201808026	54	360	280	0.0037±0.0012	-0.0012±0.0037	0.0035±0.0002	-0.0047**
	GIG201808047	54	354	286	0.0041±0.0012	-0.0007±0.0036		-0.0042**
C_{12}	GIG201808020	79	559	409	0.0108±0.0011	0.0076±0.0026		0.0026*
	GIG201808027	54	356	282	0.0215±0.0012	0.0168±0.0035	0.0050±0.0001	0.0118 X
	GIG201808048	54	350	291	0.0117±0.0012	0.0071±0.0034		0.0021*

[a] Total number of consecutive PCGC runs performed. [b] Calculated through concentration (determined by GC-FID, previously) and injection volume.

[c] CO_2 was measured manometrically after combustion. [d] Corrected by DC and MC blank mass. [e] Original Fm values were described in Table S1

[f] deviations of corrected Fm values from original Fm values. * represent the deviations are smaller than 1σ uncertainties; ** represent the deviations are smaller than 2σ uncertainties; X represent the deviations are larger than 2σ uncertainties. [g] nd, no data.

Text S8. Sampling site and air mass source regions

The city of Heshan is in the southwest of Peral River Delta (PRD) (Figure S10). The sampling site was positioned in Heshan Atmospheric Environmental Monitoring Superstation (22.711° N, 112.927° E), a rural site located at Hua Guo mountain (60m above the sea level), approximately 50 km southwest to the megacity of Guangzhou in the central Pearl River Delta (PRD). The surrounding area of the site are dominated by farmlands and forests and is far from any local anthropogenic emissions.[12,13] The air mass transport regime governing the HS station is dominated by either southerly or northerly winds. Under northeast wind regime, HS station can be well representative of air pollution outflow from the polluted central PRD region.[14] On the contrary, northeast wind regime brought clean air masses from South China Sea into PRD, which results the mixture of local emission with relatively clean oceanic air masses over HS site.

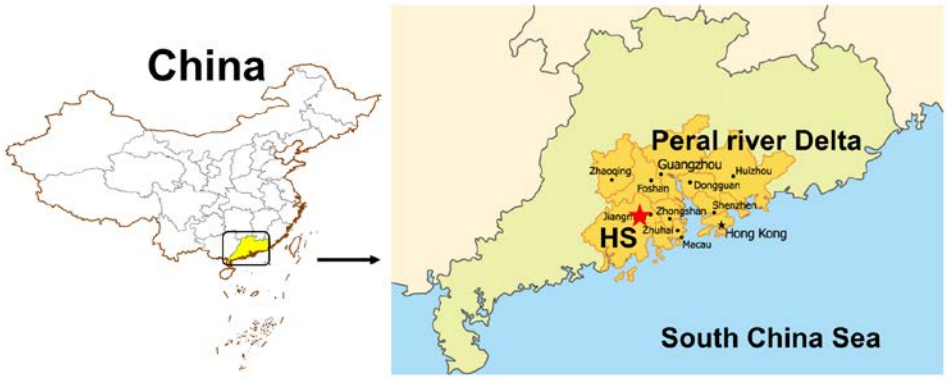

Figure S10. Map of the sampling site Heshan (HS).

To better understand the influences of air mass source regions on the constrained ^{14}C isotope composition of oxalic acid, 3-day back trajectories were performed for each of the samples using the Hybrid Single-Particle Lagrangian Integrated Trajectory (HYSPLIT4) model from the NOAA ARL website (http://ready.arl.noaa.gov/HYSPLIT.php) (Figure S11). The aerosol samples, collected under very different atmospheric transport regimes showed significantly different concentration as well as $^{13}C/^{14}C$ isotope composition of oxalic acid (Table S4).

Figure S12 shows an example HRGC trace for ambient aerosol samples before and after PCGC isolation.

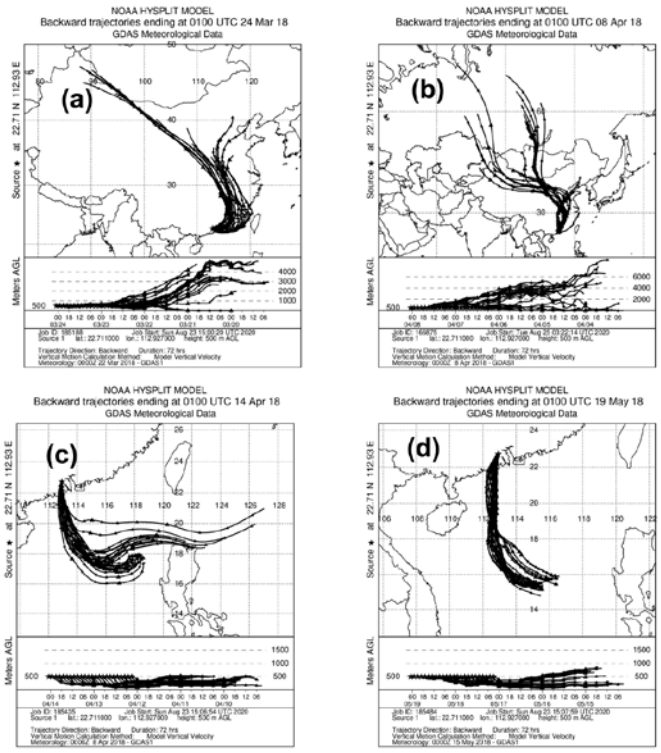

Figure S11. Three-day backward trajectory analyses for sample collected over Heshan during (a)March 22-24, 2018; (b) April 6-8, 2018 (c)April 12-14, 2018; and (d) May 17-19, 2018. Backward trajectories at 500 m over Heshan for every 2h were drawn with the NOAA HYSPLIT model.

Table S4. ^{13}C and ^{14}C isotope composition of oxalic acid in ambient aerosols in Heshan city, South China, with very different atmospheric transport sources.

Air mass source	Sampling date	C_{field} (ng m^{-3})[a]	$\delta^{13}C$ (‰)	$f_{non\text{-}fossil}$ (%)[b]	$C_{non\text{-}fossil}$ (ng m^{-3})[c]
China inland	22-24 Mar, 2018	550.0	-25.4±0.1	26.7±4.0	146.7
	6-8 Apr, 2018	703.2	-21.7±0.2	21.7±2.5	152.8
South China Sea	12-14 Apr, 2018	214.5	-14.6±0.2	77.4±1.7	166.1
	17-19 May,2018	253.9	-19.2±0.3	66.3±4.5	168.4

[a] Oxalic acid concentration in field observation. Concentrations of the oxalic acid reported here are corrected for field blanks, but are not corrected for recovery efficiencies. [b] $f_{non\text{-}fossil}$ denotes the fraction of contemporary carbon; fraction of modern carbon (Fm) was converted into the $f_{non\text{-}fossil}$ by normalization with a conversion factor of 1.06[15]. [c] $C_{non\text{-}fossil} = C_{field} \times f_{non\text{-}fossil}$.

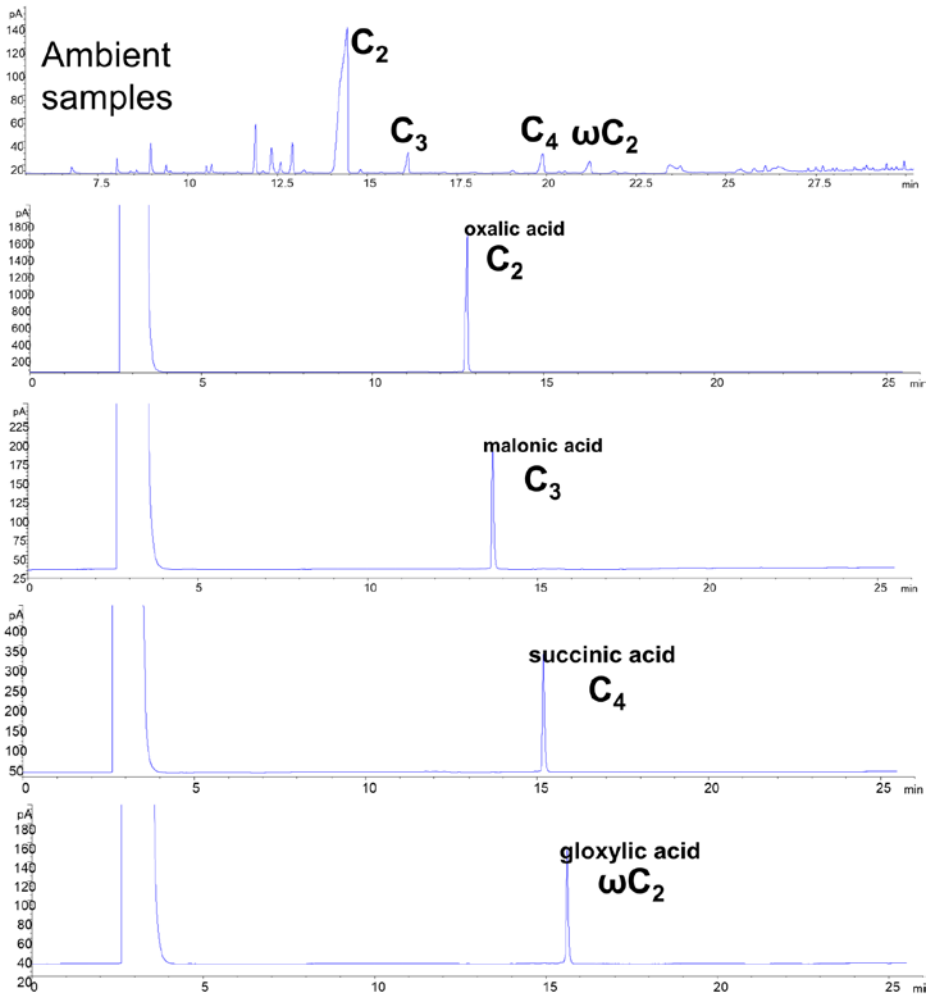

Figure S12. HRGC traces of individual ambient diacids isolated by PCGC (collected over Hehsan during March 22-24, 2018). Top trace shows initial mixture before PCGC.

Reference

(1) Casanova, E.; Tdj, K.; Williams, C.; Crump, M. P.; Evershed, R. P. Use of a 700 MHz NMR microcryoprobe for the identification and quantification of exogenous carbon in compounds purified by preparative capillary gas chromatography for radiocarbon determinations. *Anal. Chem.* **2017,** *89*, 7090−7098, 10.1021/acs.analchem.7b00987

(2) Ziolkowski, L. A.; Druffel, E. R. Quantification of extraneous carbon during compound specific radiocarbon analysis of black carbon. *Anal. Chem.* **2009,** *81*, (24), 10156, 10.1021/ac901922s

(3) Casanova, E.; Tdj, K.; Williams, C.; Crump, M. P.; Evershed, R. P. Practical considerations in high-precision compound-specific radiocarbon analyses: eliminating the effects of solvent and sample cross-contamination on accuracy and precision. *Anal. Chem.* **2018,** *90*, 11025−11032, 10.1021/acs.analchem.8b02713

(4) Kawamura, K.; Watanabe, T. Determination of stable carbon isotopic compositions of low molecular weight dicarboxylic acids and ketocarboxylic acids in atmospheric aerosol and snow samples. *Anal. Chem.* **2004,** *76*, (19), 5762-5768, 10.1021/ac049491m

(5) Eglinton, T. I.; Aluwihare, L. I.; Bauer, J. E.; Druffel, E. R. M.; Mcnichol, A. P. Gas Chromatographic Isolation of Individual Compounds from Complex Matrices for Radiocarbon Dating. *Anal. Chem.* **1996,** *68*, (5), 904-12, 10.1021/ac9508513

(6) Zencak, Z.; Reddy, C. M.; Teuten, E. L.; Xu, L.; Mcnichol, A. P.; Gustafsson, O. Evaluation of gas chromatographic isotope fractionation and process contamination by carbon in compound-specific radiocarbon analysis. *Anal. Chem.* **2007,** *79*, (5), 2042-9, 10.1021/ac061821a

(7) Hayes, J. M.; Freeman, K. H.; Popp, B. N.; Hoham, C. H. Compound-specific isotopic analyses: A novel tool for reconstruction of ancient biogeochemical processes. *Org. Geochem.* **1990,** *16*, (4), 1115-1128, https://doi.org/10.1016/0146-6380(90)90147-R

(8) Ricci, M. P.; Merritt, D. A.; Freeman, K. H.; Hayes, J. M. Acquisition and processing of data for isotope-ratio-monitoring mass spectrometry. *Org. Geochem.* **1994,** *21*,

(6), 561-571, https://doi.org/10.1016/0146-6380(94)90002-7

(9) Bour, A. L.; Walker, B. D.; Broek, T. A. B.; McCarthy, M. D. Radiocarbon Analysis of Individual Amino Acids: Carbon Blank Quantification for a Small-Sample High-Pressure Liquid Chromatography Purification Method. *Anal. Chem.* **2016,** *88*, (7), 3521-3528, 10.1021/acs.analchem.5b03619

(10) Santos, G. M.; Southon, J. R.; Drenzek, N. J.; Ziolkowski, L. A.; Druffel, E.; Xu, X.; Zhang, D.; Trumbore, S.; Eglinton, T. I.; Hughen, K. A. Blank Assessment for Ultra-Small Radiocarbon Samples: Chemical Extraction and Separation Versus AMS. *Radiocarbon* **2016,** *52*, (03), 1322-1335, 10.1017/s0033822200046415

(11) Ishikawa, N. F.; Itahashi, Y.; Blattmann, T. M.; Takano, Y.; Ogawa, N. O.; Yamane, M.; Yokoyama, Y.; Nagata, T.; Yoneda, M.; Haghipour, N.; Eglinton, T. I.; Ohkouchi, N. Improved Method for Isolation and Purification of Underivatized Amino Acids for Radiocarbon Analysis. *Anal. Chem.* **2018,** *90*, (20), 12035-12041, 10.1021/acs.analchem.8b02693

(12) Peng, J. F.; Hu, M.; Wang, Z. B.; Huang, X. F.; Kumar, P.; Wu, Z. J.; Guo, S.; Yue, D. L.; Shang, D. J.; Zheng, Z.; He, L. Y. Submicron aerosols at thirteen diversified sites in China: size distribution, new particle formation and corresponding contribution to cloud condensation nuclei production. *Atmospheric Chemistry and Physics* **2014,** *14*, (18), 10249-10265, 10.5194/acp-14-10249-2014

(13) Yuan, J. F.; Huang, X. F.; Cao, L. M.; Cui, J.; Zhu, Q.; Huang, C. N.; Lan, Z. J.; He, L. Y. Light absorption of brown carbon aerosol in the PRD region of China. *Atmospheric Chemistry and Physics* **2016,** *16*, (3), 1433-1443, 10.5194/acp-16-1433-2016

(14) Kong, L.; Hu, M.; Tan, Q.; Feng, M.; Qu, Y.; An, J.; Zhang, Y.; Liu, X.; Cheng, N. Aerosol optical properties under different pollution levels in the Pearl River Delta (PRD) region of China. *J Environ Sci (China)* **2020,** *87*, 49-59, 10.1016/j.jes.2019.02.019

(15) Liu, J.; Li, J.; Zhang, Y.; Liu, D.; Ding, P.; Shen, C.; Shen, K.; He, Q.; Ding, X.; Wang, X.; Chen, D.; Szidat, S.; Zhang, G. Source apportionment using radiocarbon and organic tracers for PM2.5 carbonaceous aerosols in Guangzhou, South China:

contrasting local- and regional-scale haze events. *Environ. Sci. Technol.* **2014,** *48*, (20), 12002-11, 10.1021/es503102w